Supporting Information

Theoretical approach to evaluate the gas-sensing performance of graphene nanoribbon/oligothiophene composites

Ayesha Ashraf [a,b], John M. Herbert [b], Shabbir Muhammad [c], Bilal Ahmad Farooqi [a], Umar Farooq [a], Muhammad Salman [a] , Khurshid Ayub [d*]

[a]Institute of Chemistry, University of the Punjab, Quaid-e-Azam Campus, Lahore, 54590 Pakistan

[b]Department of Chemistry and Biochemistry, The Ohio State University, Columbus, Ohio 43210, USA.

[c]Department of Physics, College of Science, King Khalid University, Abha, 61413, P.O. Box 9004, Saudi Arabia

[d]Department of Chemistry, COMSATS University Islamabad, Abbottabad Campus, Abbottabad, 22060, Pakistan.

***Correspondence**

Phone: +92-992-383591-6

Fax: +92-992-383441

khurshid@cuiatd.edu.pk

[1]

[1] Present Address: Institute of Chemistry, University of the Punjab, Quaid-e-Azam Campus, Lahore 54590, Pakistan

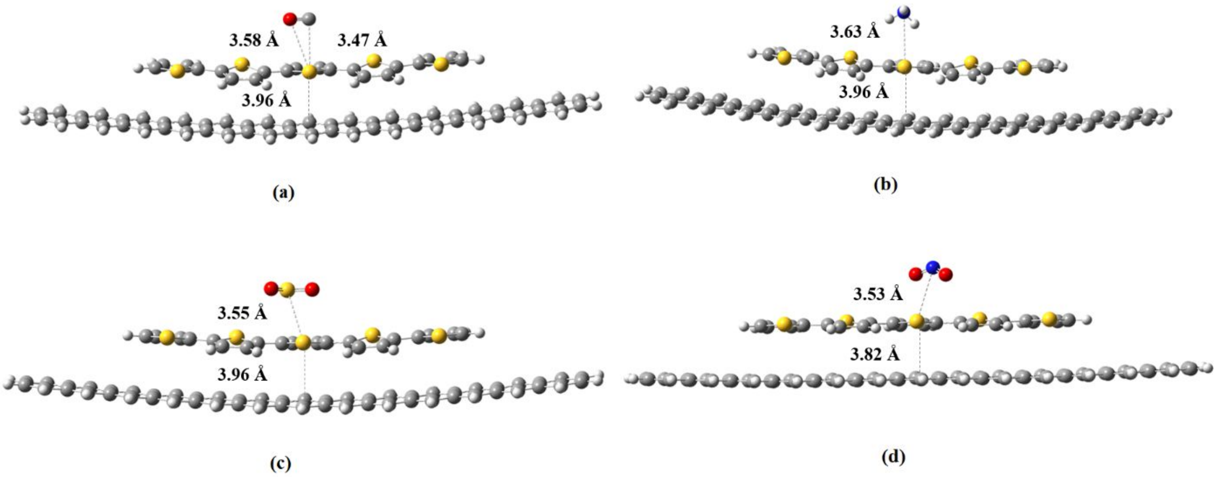

Figure S1: Optimized geometries of (a) $C_{54}H_{30}$ … 5PT … CO, (b) $C_{54}H_{30}$ … 5PT … NH_3, (c) $C_{54}H_{30}$ … 5PT … SO_2 and (d) $C_{54}H_{30}$ … 5PT … NO_2 composite-analyte complexes

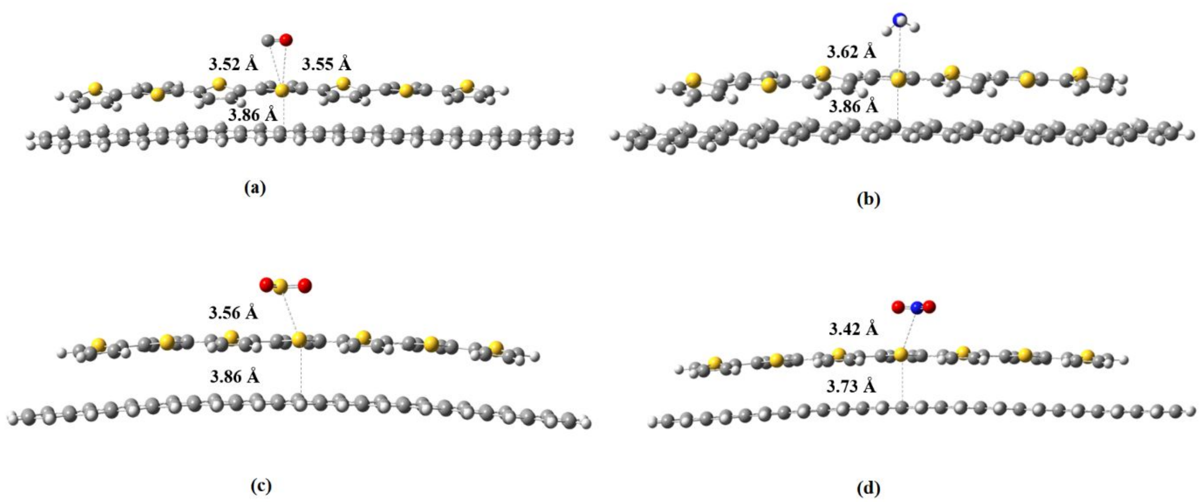

Figure S2: Optimized geometries of (a) $C_{54}H_{30}$ … 7PT … CO, (b) $C_{54}H_{30}$ … 7PT … NH_3, (c) $C_{54}H_{30}$ … 7PT … SO_2 and (d) $C_{54}H_{30}$ … 7PT … NO_2 composite-analyte complexes

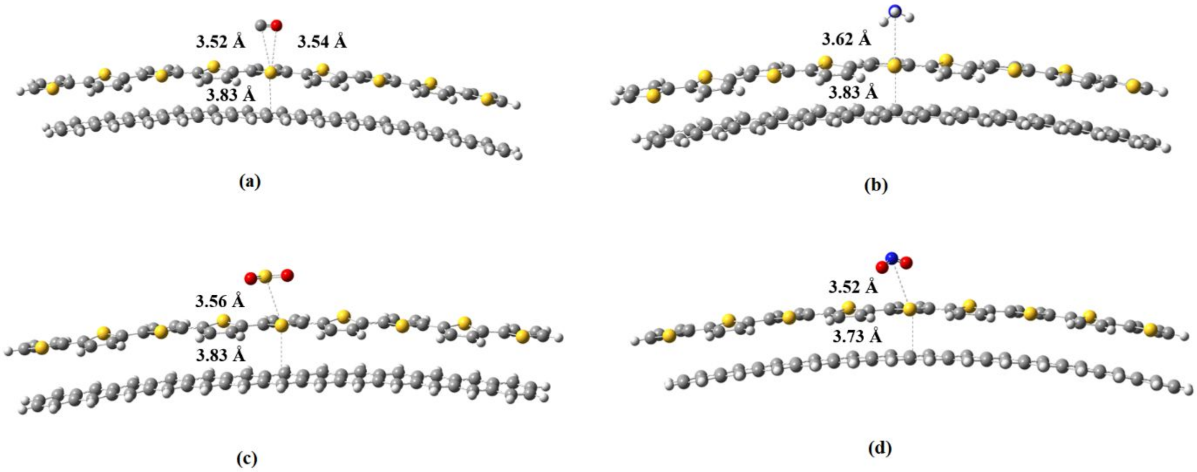

Figure S3: Optimized geometries of (a) $C_{54}H_{30}$ … 9PT … CO, (b) $C_{54}H_{30}$ … 9PT … NH_3, (c) $C_{54}H_{30}$ … 9PT … SO_2 and (d) $C_{54}H_{30}$ … 9PT … NO_2 composite-analyte complexes

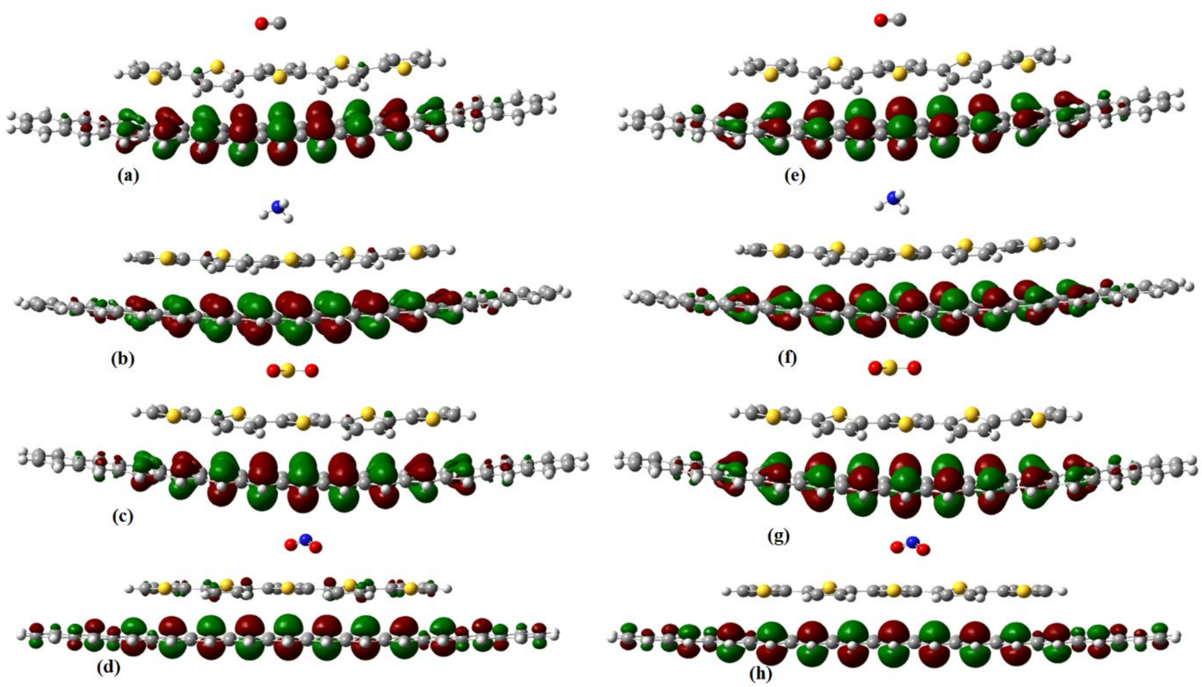

Figure S4: HOMO and LUMO orbitals of (a, e) $C_{54}H_{30}$ … 5PT … CO, (b, f) $C_{54}H_{30}$ … 5PT … NH_3, (c, g) $C_{54}H_{30}$ … 5PT … SO_2 and (d, h) $C_{54}H_{30}$ … 5PT … NO_2 composite-analyte complexes

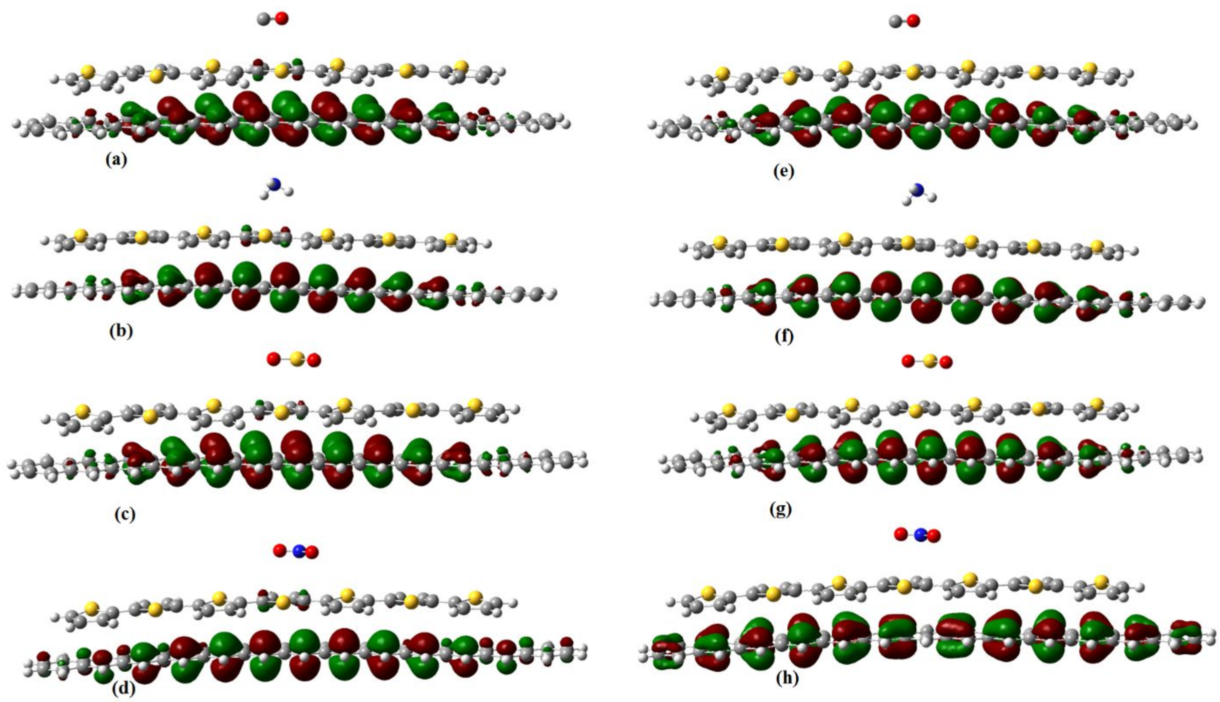

Figure S5: HOMO and LUMO orbitals of (a, e) $C_{54}H_{30}$ … 7PT … CO, (b, f) $C_{54}H_{30}$ … 7PT … NH_3, (c, g) $C_{54}H_{30}$ … 7PT … SO_2 and (d, h) $C_{54}H_{30}$ … 7PT … NO_2 composite-analyte complexes

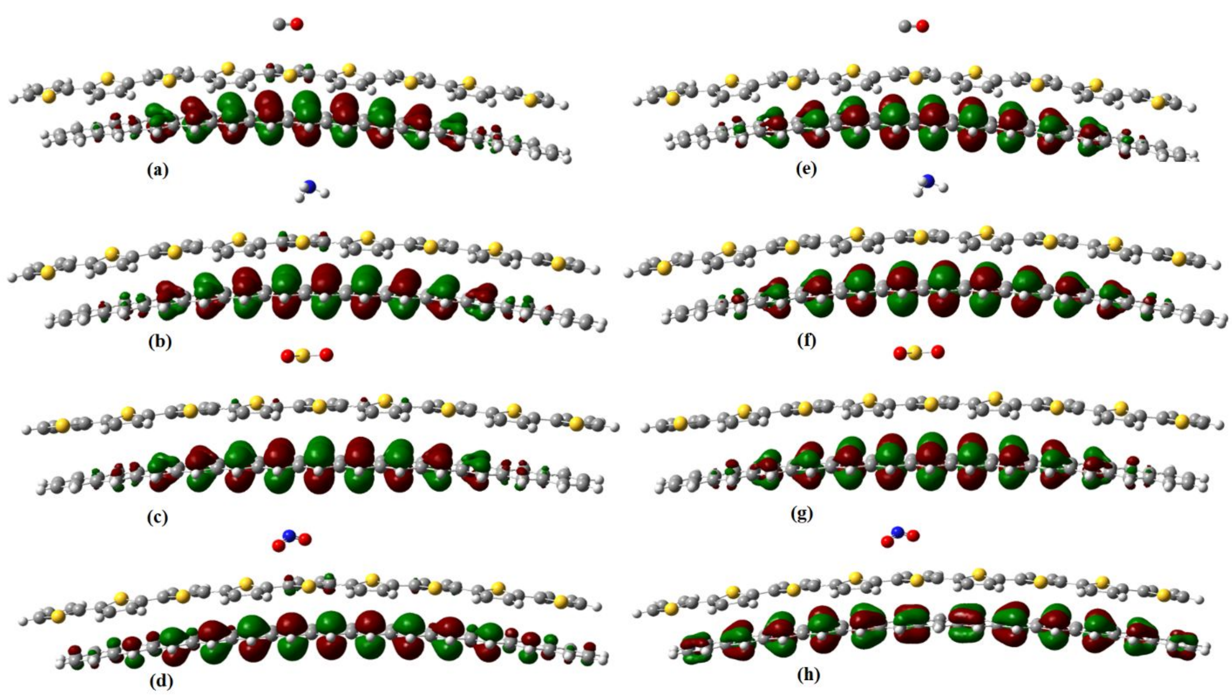

Figure S6: HOMO and LUMO orbitals of (a, e) $C_{54}H_{30}$ … 9PT … CO, (b, f) $C_{54}H_{30}$ … 9PT … NH_3, (c, g) $C_{54}H_{30}$ … 9PT … SO_2 and (d, h) $C_{54}H_{30}$ … 9PT … NO_2 composite-analyte complexes

Table S1: Ionization energy, electron affinity, chemical potential (μ), hardness (ŋ), softness (S), and electrophilicity (ω) of $C_{54}H_{30}$ … nPT … CO, $C_{54}H_{30}$ … nPT … NH_3, $C_{54}H_{30}$ … nPT … SO_2 and $C_{54}H_{30}$ … nPT … NO_2 (n= 3, 5, 7, 9) composite-analyte complexes

System	I.E	E.A	Chemical Potential (μ)	Softness (S)	Hardness (η)	Electrophilicity (*ω*)
$C_{54}H_{30}$...3PT	3.86	3.22	-3.54	1.58	0.32	19.80
$C_{54}H_{30}$...3PT…CO	3.88	3.23	-3.55	1.54	0.32	19.47
$C_{54}H_{30}$...3PT…NH_3	3.92	3.27	-3.59	1.54	0.32	19.92
$C_{54}H_{30}$...3PT…SO_2	3.92	3.29	-3.61	1.60	0.31	20.85
$C_{54}H_{30}$...3PT…NO_2	4.45	2.56	-3.51	0.53	0.94	6.51
$C_{54}H_{30}$...5PT	3.78	3.19	-3.48	1.71	0.29	20.67
$C_{54}H_{30}$...5PT…CO	3.79	3.19	-3.49	1.69	0.30	20.62
$C_{54}H_{30}$...5PT…NH_3	3.83	3.24	-3.53	1.69	0.30	21.14
$C_{54}H_{30}$...5PT…SO_2	3.82	3.23	-3.53	1.91	0.30	21.04
$C_{54}H_{30}$...5PT…NO_2	4.28	2.62	-3.45	0.60	0.83	7.18
$C_{54}H_{30}$...7PT	3.77	3.19	-3.48	1.72	0.29	20.77
$C_{54}H_{30}$...7PT…CO	3.78	663	-3.49	1.72	0.29	20.86
$C_{54}H_{30}$...7PT…NH_3	3.81	3.23	-3.52	1.72	0.29	21.26
$C_{54}H_{30}$...7PT…SO_2	3.82	3.24	-3.53	1.72	0.29	21.42
$C_{54}H_{30}$...7PT…NO_2	4.03	3.19	-3.61	1.19	0.42	15.53
$C_{54}H_{30}$...9PT	3.76	3.18	-3.47	1.73	0.29	20.79
$C_{54}H_{30}$...9PT…CO	3.77	3.19	-3.48	1.73	0.29	20.91
$C_{54}H_{30}$...9PT…NH_3	3.81	3.22	-3.52	1.72	0.29	21.28
$C_{54}H_{30}$...9PT…SO_2	3.80	3.21	-3.51	1.72	0.29	21.16
$C_{54}H_{30}$...9PT…NO_2	4.01	3.39	-3.70	1.63	0.31	22.38

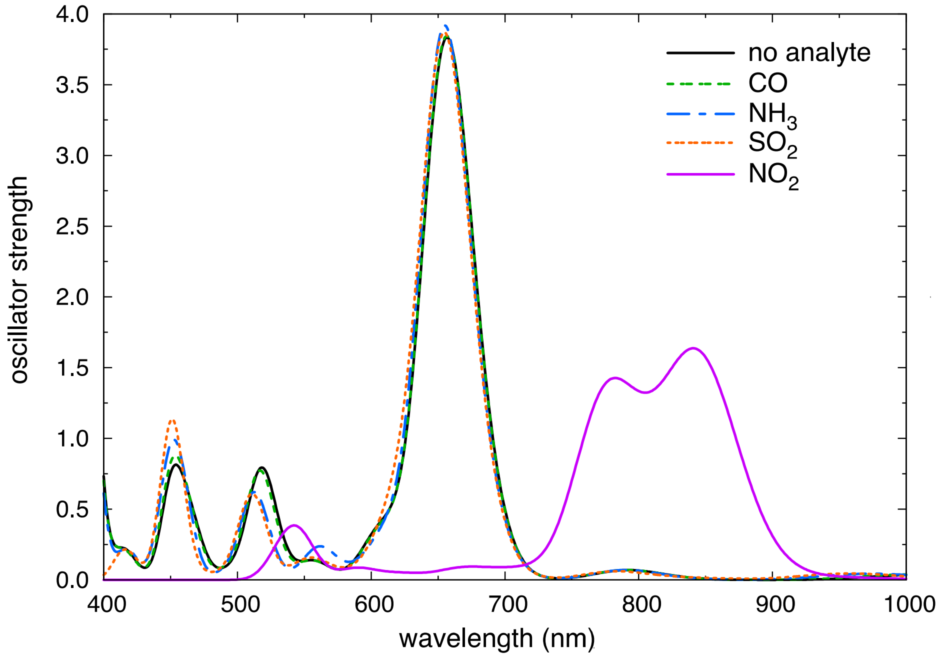

Figure S7: UV-vis spectra of $C_{54}H_{30}$ … 5PT, $C_{54}H_{30}$ … 5PT… CO, $C_{54}H_{30}$ … 5PT … NH_3, $C_{54}H_{30}$ … 5PT … SO_2 and $C_{54}H_{30}$ … 5PT … NO_2 composite-analyte complexes, computed at the TD-B3LYP/6-31G level.**

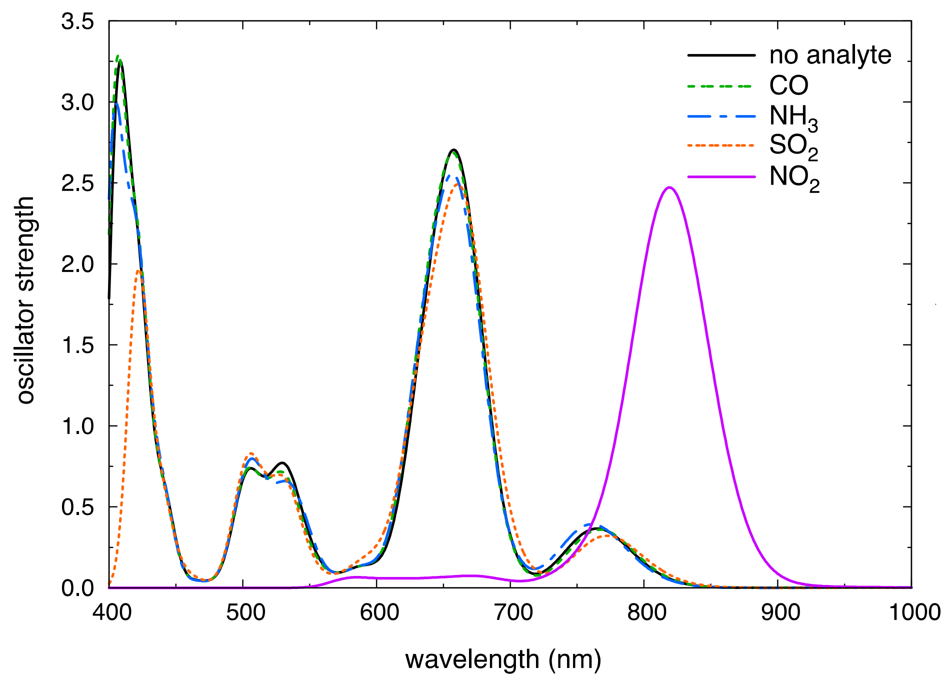

Figure S8: UV-vis spectra of $C_{54}H_{30}$ … 7PT, $C_{54}H_{30}$ … 7PT… CO, $C_{54}H_{30}$ … 7PT … NH_3, $C_{54}H_{30}$ … 7PT … SO_2 and $C_{54}H_{30}$ … 7PT … NO_2 composite-analyte complexes, computed at the TD-B3LYP/6-31G level.**

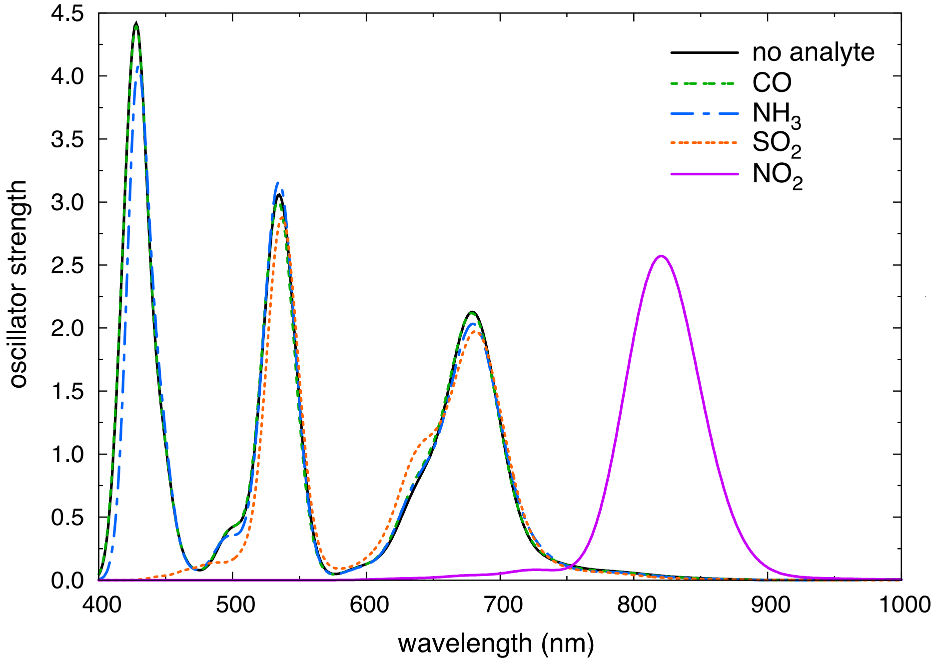

Figure S9: UV-vis spectra of $C_{54}H_{30}$ … 9PT, $C_{54}H_{30}$ … 9PT… CO, $C_{54}H_{30}$ … 9PT … NH_3, $C_{54}H_{30}$ … 9PT … SO_2 and $C_{54}H_{30}$ … 9PT … NO_2 composite-analyte complexes, computed at the TD-B3LYP/6-31G level.**

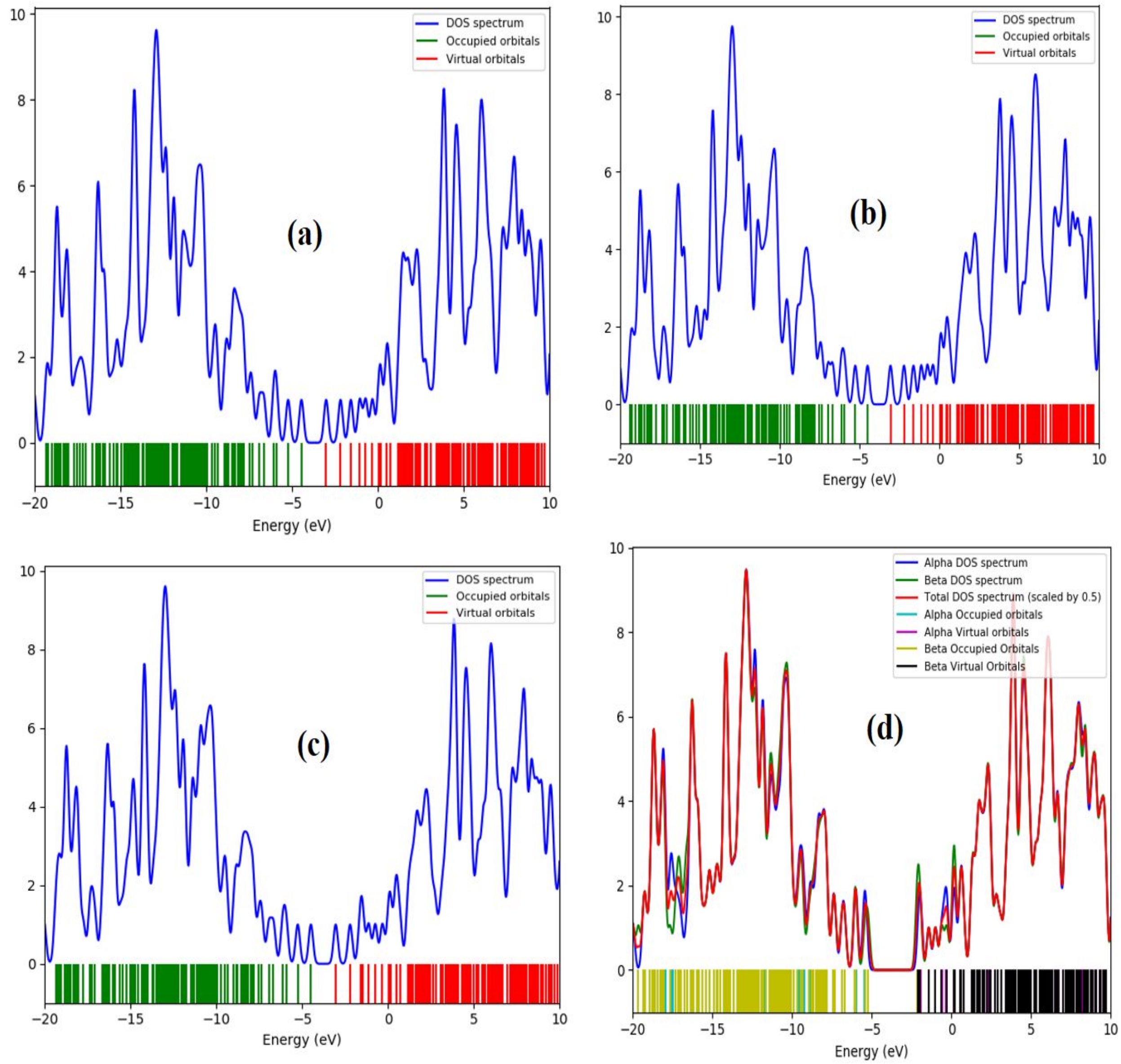

Figure S10: DOS spectra of (a) $C_{54}H_{30}$ … 5PT … CO, (b) $C_{54}H_{30}$ … 5PT … NH_3, (c) $C_{54}H_{30}$ … 5PT … SO_2 and (d) $C_{54}H_{30}$ … 5PT … NO_2 composite-analyte complexes

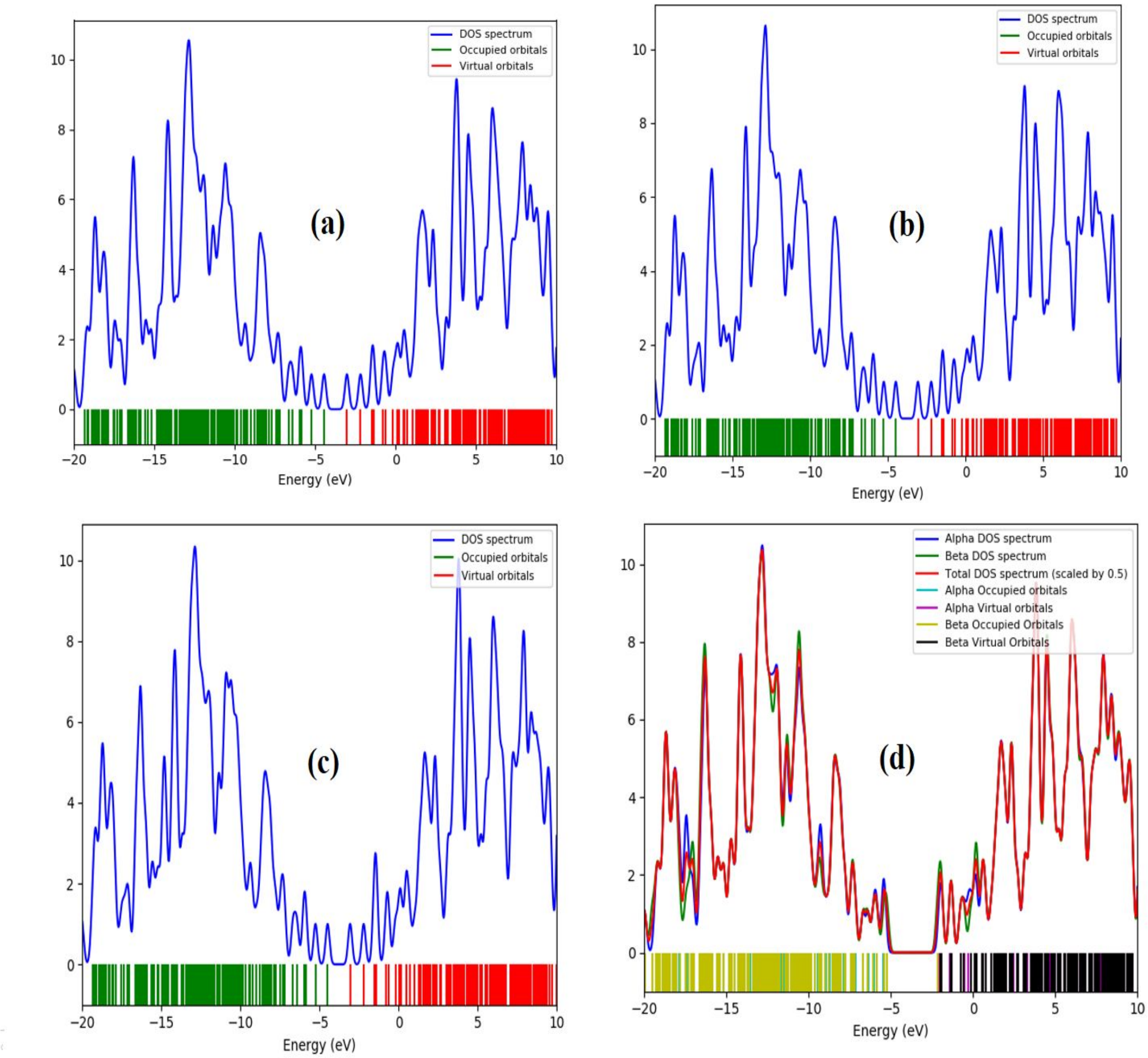

Figure S11: DOS spectra of (a) $C_{54}H_{30}$ … 7PT … CO, (b) $C_{54}H_{30}$ … 7PT … NH_3, (c) $C_{54}H_{30}$ … 7PT … SO_2 and (d) $C_{54}H_{30}$ … 7PT … NO_2 composite-analyte complexes

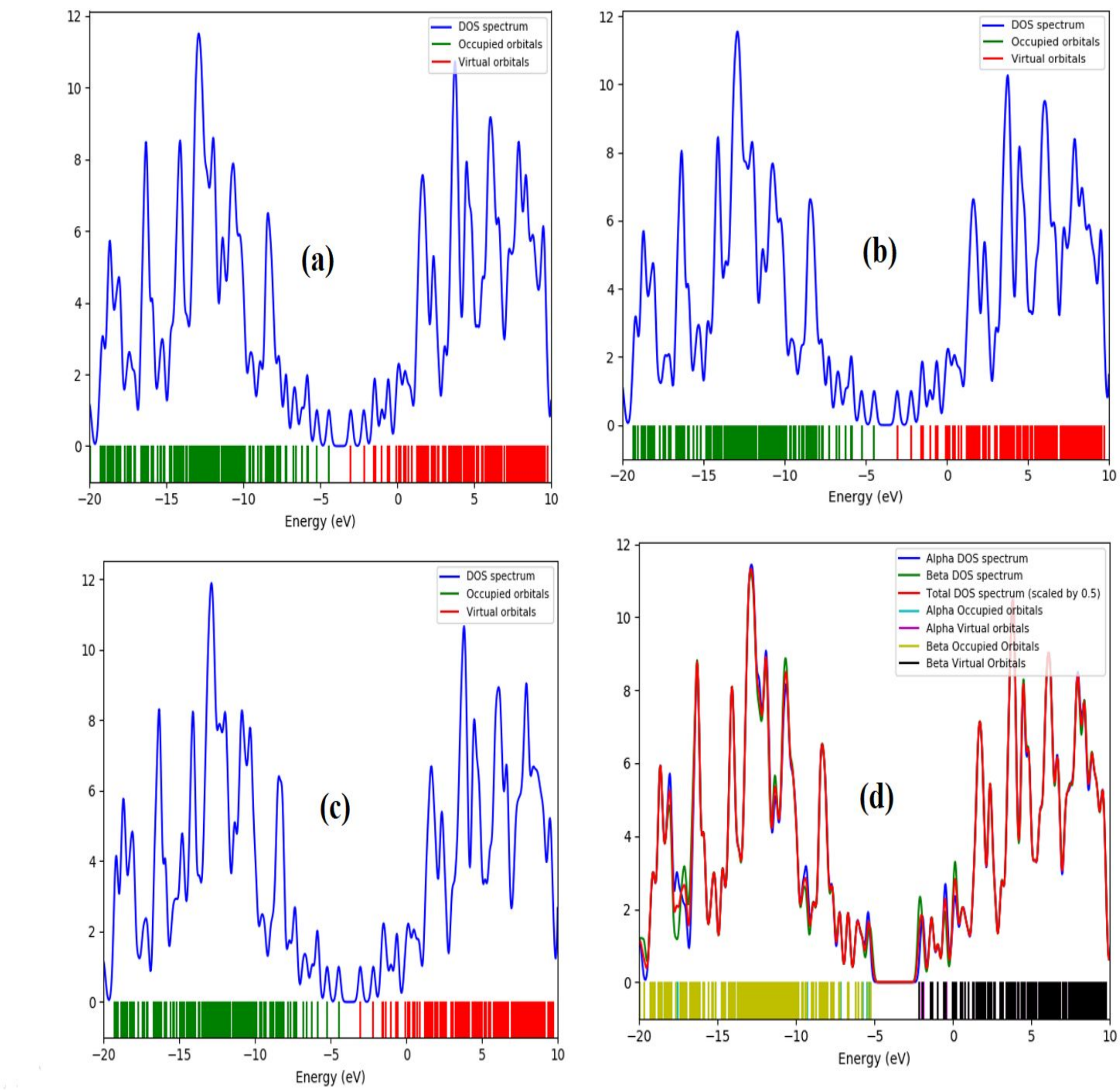

Figure S12: DOS spectra of (a) $C_{54}H_{30}$ … 9PT … CO, (b) $C_{54}H_{30}$ … 9PT … NH_3, (c) $C_{54}H_{30}$ … 9PT … SO_2 and (d) $C_{54}H_{30}$ … 9PT … NO_2 composite-analyte complexes

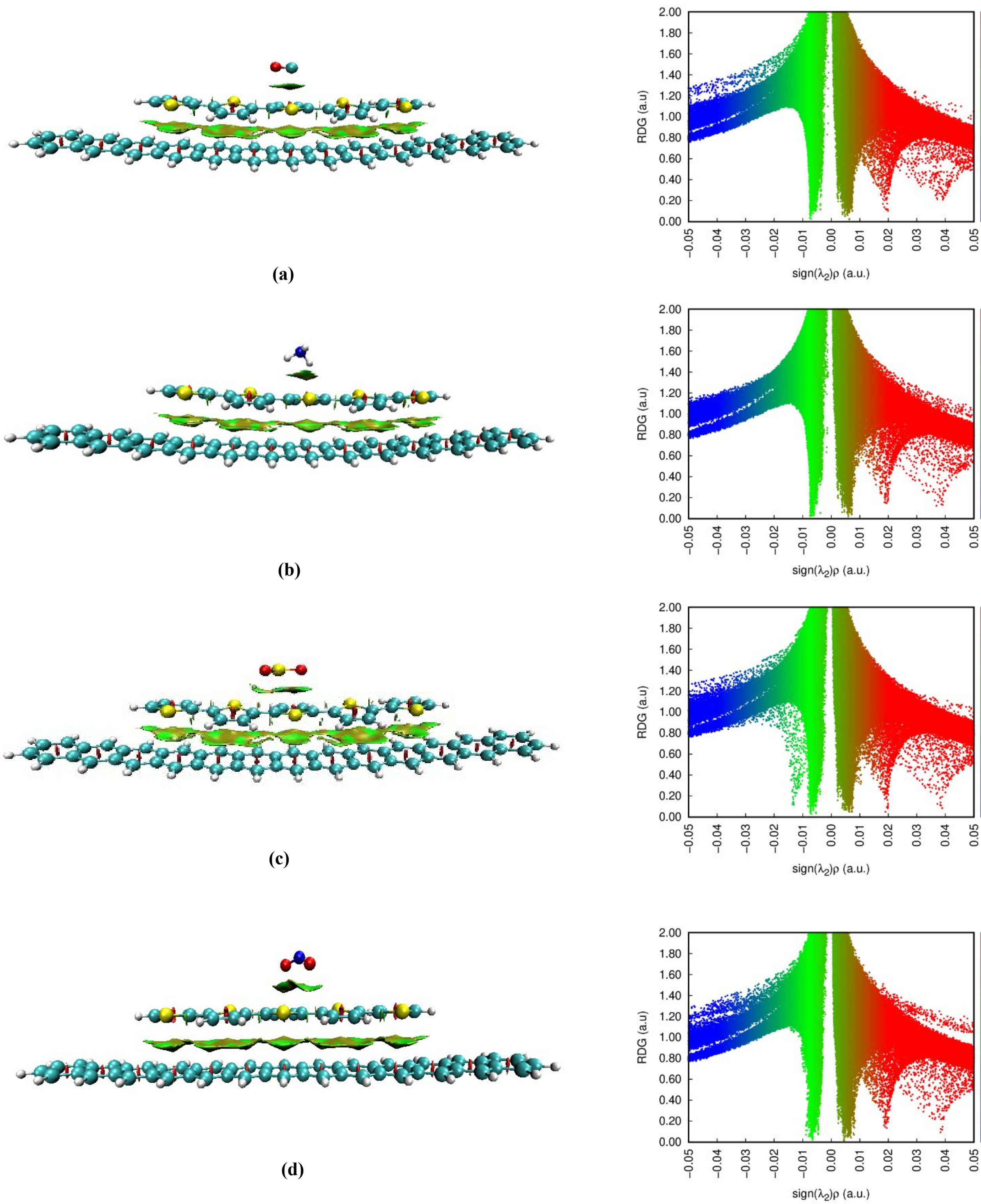

Figure S13: Color-mapped RDG isosurface graphs (3D) and scatter diagrams (2D) of (a) $C_{54}H_{30}$ … 5PT … CO, (b) $C_{54}H_{30}$ … 5PT … NH_3, (c) $C_{54}H_{30}$ … 5PT … SO_2 and (d) $C_{54}H_{30}$ … 5PT … NO_2 composite-analyte complexes

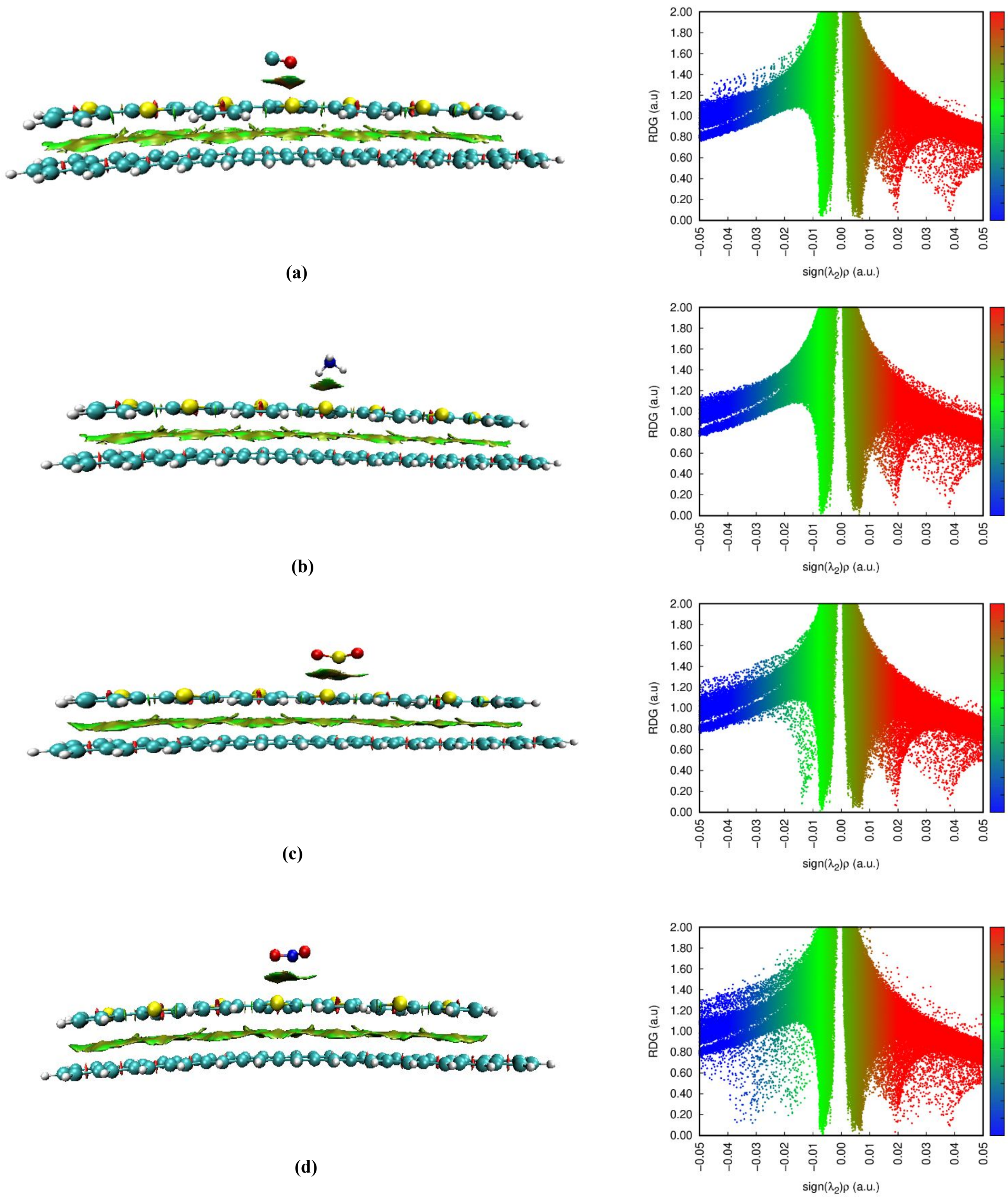

Figure S14: Color-mapped RDG isosurface graphs (3D) and scatter diagrams (2D) of (a) $C_{54}H_{30}$ … 7PT … CO, (b) $C_{54}H_{30}$ … 7PT … NH_3, (c) $C_{54}H_{30}$ … 7PT … SO_2 and (d) $C_{54}H_{30}$ … 7PT … NO_2 composite-analyte complexes

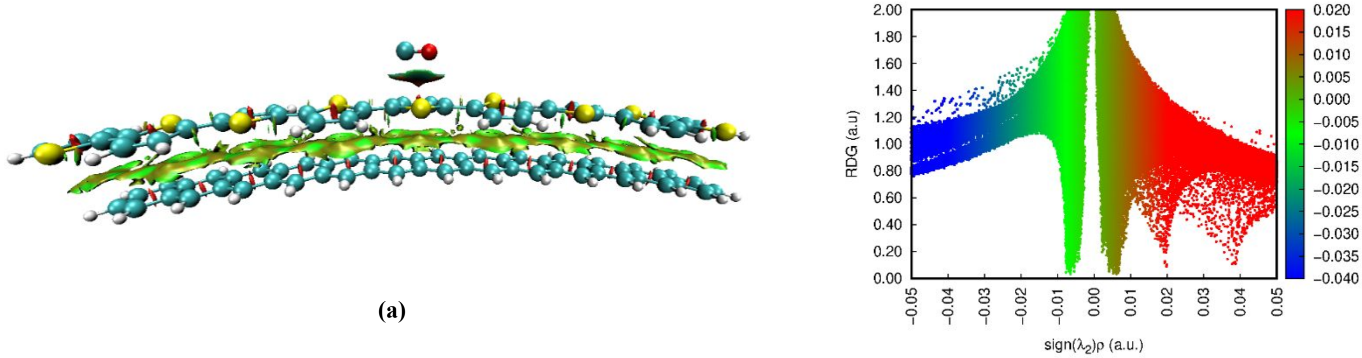

(a)

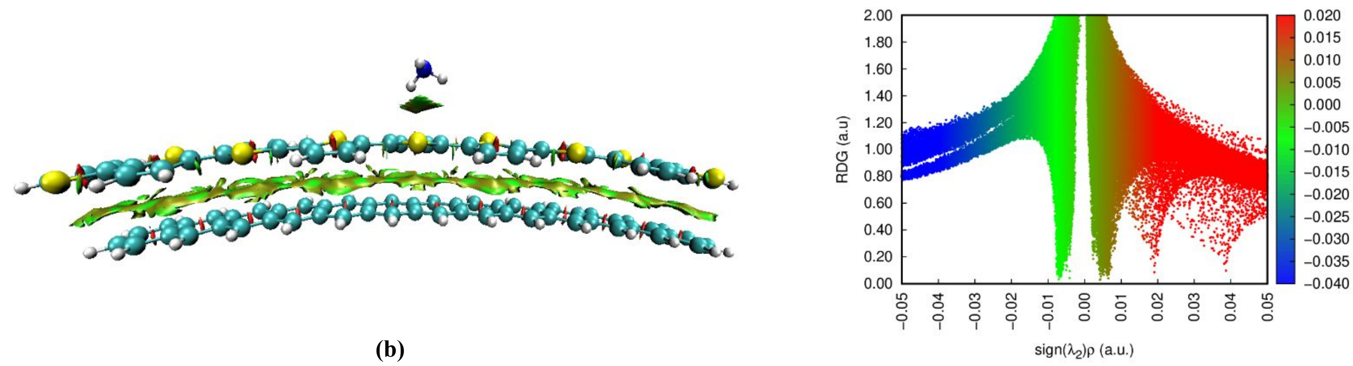

(b)

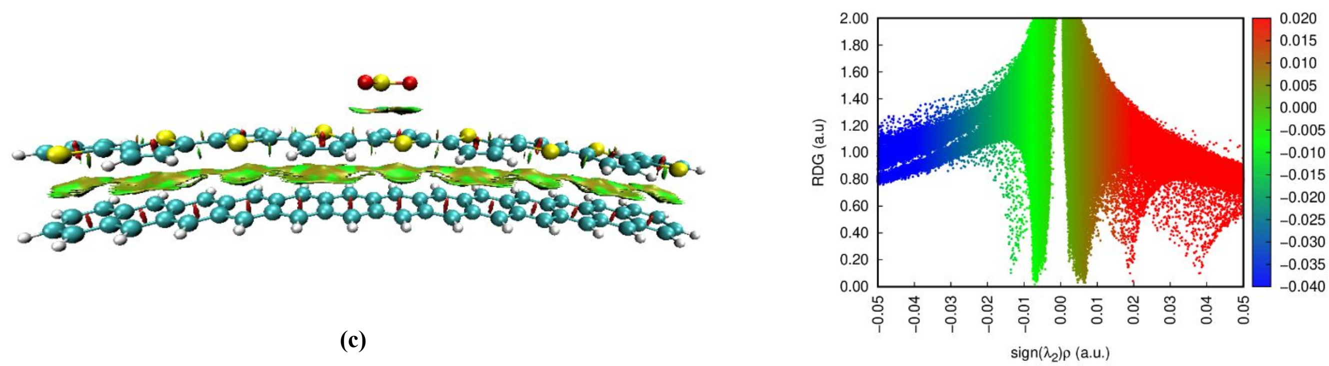

(c)

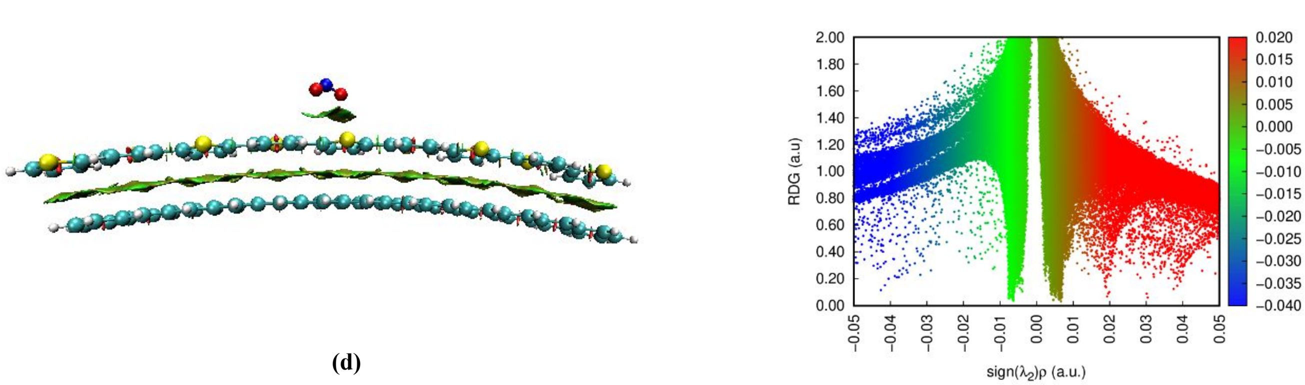

(d)

Figure S15: Color-mapped RDG isosurface graphs (3D) and scatter diagrams (2D) of (a) $C_{54}H_{30}$ … 9PT … CO, (b) $C_{54}H_{30}$ … 9PT … NH_3, (c) $C_{54}H_{30}$ … 9PT … SO_2 and (d) $C_{54}H_{30}$ … 9PT … NO_2 composite-analyte complexes